Theses and Dissertations

2016

Adaptive Critic Design based Cooperative Control for Pulsed Power Loads Accommodation in Shipboard Power System

Liang Tan
Lehigh University

Follow this and additional works at: http://preserve.lehigh.edu/etd

Part of the Electrical and Computer Engineering Commons

Adaptive Critic Design based Cooperative Control for Pulsed Power Loads Accommodation in Shipboard Power System

By

Liang Tan

A Thesis

Presented to the Graduate and Research Committee

of Lehigh University

in Candidacy for the Degree of

Master of Science

in

Electrical and Computer Engineering

Lehigh University

2 May, 2016

Thesis is accepted and approved in partial fulfillment of the requirements for the Master of Science in Electrical and Computer Engineering.

Cooperative optimal control for pulsed power loads accommodation in shipboard power system
Liang Tan

_____

Date Approved

_____

Wenxin Liu
Thesis Advisor

_____

Filbert J. Bartoli
Department Chair Person

Acknowledgements

My thanks go out to the Lehigh professors who have helped nurture my desire to learn, and helped me learn lessons, both academic and in life that I will keep with me for the rest of my life.

Thanks specifically go out to Professor Wenxin Liu, who has both been an incredible instructor and mentor. Without his guidance and support during the period of pursuing the degree, I could not go through the projects and grasp the critical concepts of electrical engineering.

Thanks also should go to Dr Im Wonsang from my lab. As a talented electrical engineer, he is so inspirational and supportive throughout the duration of my project: he held rigorous attitude toward each detail and always kept my spirits up by giving insightful advice on my design. Studying with him is a precious experience during my stay at Lehigh University, and has set up a great example for doing research and also being great person.

Finally, I thank my family for their continuous support, inspiring encouragement and unconditional love; and friends, both at Lehigh and abroad for their support and encouragement through my undergraduate and graduate education.

Table of Contents

List of figures

List of tables

Abstract

Since a pulsed power load (PPL) consumes a huge amount of energy within very short period of time, its deployment might cause large disturbances even instability to a power system that has limited generation, small inertia, and small ramp rate. To mitigate the strike during PPL deployment, energy storage system (ESS) is usually installed in shipboard power system (SPS) to serve as the sole power supply for PPL. To realize fast charging of the ESS and minimize disturbance during charging, generation control and charging control of SPS should be well coordinated. For this important but not well studied problem, this paper presents an adaptive critic design based control algorithm for a nonlinear model integrating the basic dynamics of synchronous generator and supercapacitor, which is a popular type of ESS for PPL application. Through interactive learnings of two neural networks for cost-to-go function approximation and optimal control approximation, respectively, near optimal control can be realized even under disturbance and model impreciseness. The algorithm is tested with both detailed single- and multiple-generator SPS models and tested through both real-time digital and power hardware-in-the-loop simulations. Simulation results demonstrate the effectiveness of the developed model and control algorithm.

1. Introduction

1.1 Background

1.1.1 Shipboard power system

The shipboard power system (SPS) is a microgrid [1] consisting of multiple generators and a variety of loads. The topology of the notional MVAC SPS model developed by the Electrical Ship Research and Development Consortium (ESRDC) [2] is depicted in Fig.1.
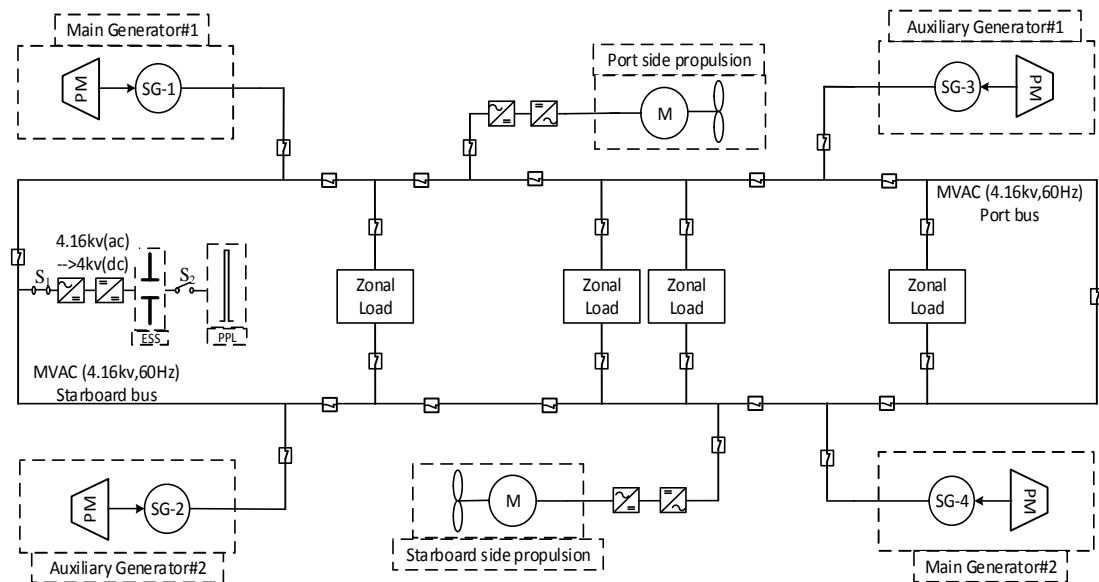
Figure 1. *Topology of the notional MVAC SPS model developed by ESRDC*

In the notational MVAC model, four generators (two main and two auxiliaries) are connected to form a 4.16 kV ac ring bus. Two Propulsion Module (PMs) are connected to the ring bus through AC/DC/AC back-to-back converters. The back-to-back converter also allows bidirectional power flow so that the PMs can feed power back to the ring bus when the PMs decelerate. The ESS that powers the PPL is connected to the ring bus through a step-down transformer and an AC/DC converter that converts the 4.16 kV ac to 4 kV dc voltages. A large number of circuit breakers are installed on both port and

starboard buses to switch the SPS between different operating modes, such as cruise mode and battle mode. The ship service loads are implemented and shown as zonal loads. More details about the model can be found in [2].

1.1.2 Pulsed power system

Nowadays, naval ships have been equipped with a variety of advanced facilities including high power radars, electromagnetic launch and recovery systems, and weapons such as rail guns, which are referred collectively as pulsed power loads (PPL) [3]. Once triggered, a PPL consumes a huge amount of energy within a very short period of time[4]. The SPS is usually designed to satisfy the loads that is online most of the time instead of meeting the peak demand of all loads. In addition to a capacity limit, it is nearly impossible to adjust generations of synchronous generators (SGs) instantaneously due to the limited generation ramp rates. If a PPL is directly connected to the SPS, the sudden demand increase could cause huge voltage sags in DC SPS and significant frequency drop in AC SPS. Under certain conditions, not only sensitive loads might be tripped offline but also system-wide instability of the SPS could be incurred [5].

1.2 Motivation

The negative impacts of PPL to SPS have been studied through simulations and analysis in [6][7][8][9][10][11]. Detailed SPS models are used to investigate the transient performance and stability of SPS under PPLs of various magnitude, duration, and frequency. Based on these studies, the first investigated solution for PPL accommodations is load management. According to the load management solution [4] [8], the loads that are less critical than PPL for a particular task or during a period of time

3

are shed to meet the high power demand of PPL. As can be imagined, the load management solution will cause degraded or interrupted service. Even if SPS's generation after load management can meet the peak demand of the PPL, the generation might not be able to satisfy the ramp rate requirement of the PPL.

The second solution for PPL accommodation is installing specialized energy storage systems (ESS). The ESS charging can usually be given a decent amount of time that is much longer than the duration of PPL deployment, such as 30-second charging vs. 1-second of PPL deployment. In this way, the huge transient power demand is transformed into a mild one that can be addressed within a decent amount of time. To further reduce the negative impacts and overcome the limited ramp rate of SPS, the fully charged ESS can be disconnected from the SPS and serve as the sole power supply during PPL deployment. To handle the extreme conditions, a practical PPL solution should integrate the two solutions of ESS installation and load management.

Currently, the two most popular types of ESS for PPL applications are supercapacitor and flywheels. There have been discussions on the advantages and disadvantages of these types ESS in term of initial and maintenance costs, weight, power density, transient performance, [5] [12][13] [14] [15]. In this paper, supercapacitor is considered due to its advantages of simple maintenance, good reliability, and high power density [7] [16]. The concept of controller design can be extended to other types of ESS by considering their specific static and dynamic properties.

Even though the installation of ESS can alleviate the negative impacts of PPL to SPS, charging of the ESS still could incur large voltage or frequency disturbances if not properly handled. Among the few solutions for PPL accommodation in microgrids or SPS,

4

the leading ones are limit-based control (LBC) [17] and profile-based control (PBC) [18], which are used to generate the charging current reference for capacitor-type ESS. Both algorithms had been tested through experimentation with a medium voltage DC (MVDC) testbed. The experimental results demonstrated the effectiveness of the algorithms. However, there is still room for improvement for this important but not well studied problem. From the experimental results of LBC, one can see that there is a sudden increase of the output voltage after the capacitor gets fully charged. This is due to the immediate discontinuation of nonzero charging current. Smooth charging was considered during PBC design and the interrupted charging current becomes much smaller. In LBC and PBC, the charging current references are determined in an offline manner and held fixed after that. Since possible load changes are not considered, the charging current might become impractical during severe load increase and conservative during durative load decrease. Aggressive charging will cause large disturbance, and conservative charging will unnecessarily prolong charging duration.

1.3 Contributions and Organization

To better accommodate the PPL in SPS, improved closed-loop control algorithms that can provide fast and smooth charging are needed. This can be realized by well coordinating the charging and generation controls with sufficient consideration of uncertainties and constraints. To facilitate advanced control design, a simple SPS model is first developed. The model can represent the basic dynamics of SG and supercapacitor. Base on the model, an adaptive critic design (ACD)-based cooperative control algorithm is developed. First proposed by Werbos [19], ACD has been widely accepted as a promising practical optimal control solution for nonlinear systems in the presence of

5

noise and uncertainties [20]. In ACD-based control schemes, there are usually two neural networks (NNs), a critic NN and an action NN [21] [22] to approximate the cost-to-go function and the optimal control, respectively. Through continuously interactive learning, near optimal control can be realized even under disturbance and model impreciseness [23]. The algorithm is tested with detailed single-generator model through power hardware-in-the-loop simulation and detailed multiple-generator SPS model through real-time digital simulation. Simulation results demonstrate that the designed algorithm can provide fast and smooth charging of the ESS.

The rest of this paper is organized as follows. In Section II, a simple control model for MVAC SPS is developed. In Section III, the ACD based control algorithm for PPL accommodation is presented. In Section IV, real-time digital simulation results with both single- and multiple- generator SPS models are presented and power hardware-in-the-loop simulation results are also provided. Concluding remarks are given in Section V.

This thesis is mainly based on one of my paper accepted by *IET Generation, Transmission & Distribution.*

2. Problem Formulation

Even though the notional MVAC SPS model is very complicated, the power that flows in the system can be represented with a simplified one-generator two-loads SPS as shown in Fig.2. The SG in Fig.2 represents the aggregated model of multiple SGs. One load represents the supercapacitor for PPL accommodation, and the other load represents all other loads and losses in the system. During supercapacitor charging, S_1 is closed and S_2 is open. During PPL deployment, S_1 is open and S_2 is closed. P_M stands for the overall mechanical power input to the SG. P_C is the charging power for supercapacitor. P_L stands for all other active power loads and loss. $P_G = P_L + P_C$ is the total active power generation of the system. Since cooperative control will calculate generation and charging control references, it is unnecessary to consider too much model details. Even if the simplified model can be used for control design, the designed algorithms should be tested with detailed SPS model to evaluate the effectiveness of the developed model and algorithm.
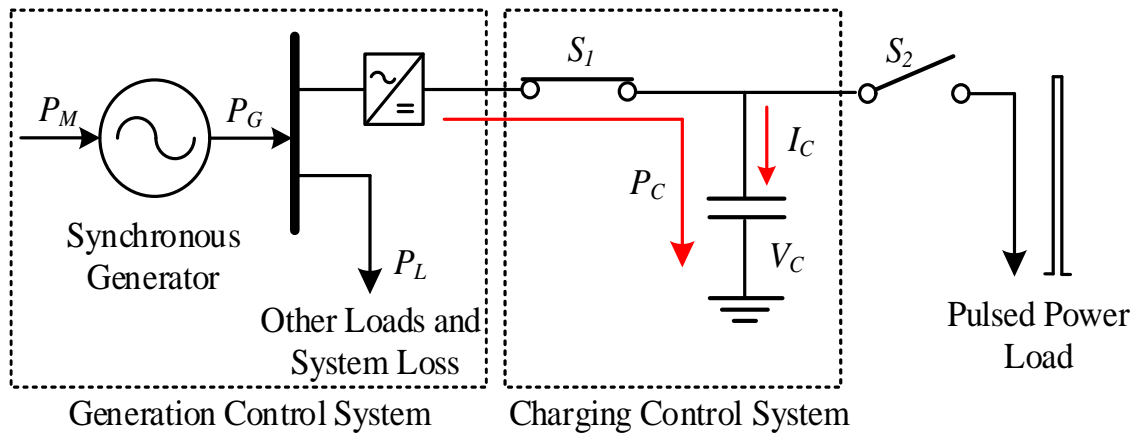
Figure 2. *Simplified SPS topology for model development*

To model the generation control system, the simple SG model shown in (1) can be used [24][25].

$$\dot{f} = k_1(P_M - P_G) = k_1(P_M - P_L - I_C V_C) \tag{1}$$

where f is the system frequency, k_1 is a constant decided by generator's parameters including the inertia constant. It is important to note that supply-demand mismatch (difference between P_M and P_G) causes system frequency oscillation. To achieve good system-wide static and dynamic performance, P_M must be properly adjusted based on demand.

The $i\text{-}v$ characteristic shown in (2) is adopted to model the charging control system by

$$\dot{V}_C = k_2 I_C \tag{2}$$

where V_C is the capacitor voltage, I_C is the charging current, and k_2 is the reciprocal of the capacitance of the supercapacitor C.

(1) and (2) together form the simplified MVAC SPS model for cooperative controller design. The model has several interesting properties from control point of view, such as being nonlinear, consisting of strongly coupled subsystems, and having multiple inputs and multiple outputs. It is true that the practical SPS model is far more complex compared to the above simplified second order model. However, a detailed model will make the control algorithm extremely difficult to design, or even is beyond the capability of existing control theory. In addition, no model can fully grasp the dynamics and nonlinearity of the complicated SPS. As demonstrated through simulation studies, the model is simple yet can represent the basic dynamics of the generators and supercapacitor on board.

In the model, f and V_C are the states as well as outputs of the system, i.e., $x=y=[f, V_C]^T$. To achieve fast ESS charging, V_C should be charged to a desired level within a short period of time. To achieve stable charging, the system frequency should be

stabilized around its nominal value of 60 Hz. The control objective can be realized by properly designing the control inputs, P_M and I_C, i.e., $u=[P_M, I_C]^T$.

Based on Euler's approximation, above continuous-time dynamic model can be discretized as

$$x[k+1] = x[k] + \begin{bmatrix} k_1 T & -k_1 T x_2[k] \\ 0 & k_2 T \end{bmatrix} u[k] + d[k]$$

$$y[k+1] = x[k+1]$$

(3)

where $x[k] = y[k] = [f[k] \quad V_C[k]]^T$, and $u[k] = [P_M[k] \quad I_C[k]]^T$. $d[k] = [d_1[k] \quad d_2[k]]^T$ stand for the bounded uncertainties, intentionally added to represent various model inaccuracy and external disturbance.

In this paper, the objective of the controller is to minimize frequency oscillations and to manipulate the output $y[k]$ to track the predefined voltage charging profile, i.e., $y_d[k] = [f[k] \quad V_d[k]]^T$. Thus, the tracking error can be readily defined as

$$e[k] = y[k] - y_d[k]$$

(4)

3. Adaptive critic design based control

3.1 Preliminaries

In this section, some necessary background on approximation property of NN and ACD are given. The proposed controller design is presented afterwards.

3.1.1: Approximation property of NN

The commonly used property of NN for control is its capability for approximation and adaptation [26]. Let x be the input vector and y be the output vector, then a general function associated with the input and output of a commonly used two-layer NN can be written as:

$$y = f(x) = W^T \Phi(V^T x) + \nu(x) = W^T \Phi(x) + \nu(x) \tag{5}$$

where V and W are the hidden layer and output layer weights, respectively.   (x) is the activation function, and   (x) is the reconstruction error.

If V is fixed, the only design parameter in the NN is W matrix and this NN becomes a simplified version of a function link network (one layer NN), which is easier to tune. It is demonstrated in [27] that, if the hidden layer weights V are chosen initially at random and held fixed while hidden-layer neurons are sufficiently large, the NN reconstruction error   (x) can be made arbitrarily small since the activation function vector forms a basis. That is the reason why $W^T \Phi(V^T x)$ is replaced by $W^T \Phi(x)$ in (5).

3.1.2: Adaptive critic design

ACD is an NN-based optimization and control technique that solves the classical nonlinear optimal control problem by combining concepts of approximate dynamic

programming (ADP) and reinforcement learning. The central idea of ACD approach is that the optimal control law and cost function are approximated by online adapting two NNs, namely, an action NN and a critic NN. Instead of finding the exact minimum, ACD utilizes the two NN to approximate the Hamilton–Jacobi–Bellman equation associated with optimal control theory [28]. The adaptation process of the two NN starts with a nonoptimal, arbitrarily chosen control by the action NN; the critic NN then guides the action NN toward the optimal solution adaptively. During the process, neither of the NNs needs any "information" of an optimal trajectory, but only the desired cost needs to be known [29]. In addition, this method does not require the difficult offline training and can be easily implemented.

To obtain the optimal control is to solve the Bellman equation that optimizes the cost-to-go function $J[k]$ of the system, which is defined as

$$J[k] = J(x[k], u) = \sum_{i=0}^{\infty} x^i r[k+i] = x J[k+1] + r[k] \tag{6}$$

where $u[k]$ is a control policy at k instant step, $x (0 \leq x \leq 1)$ is the discount factor for the infinite-horizon problem. The user- defined utility function $r[k]$ can be viewed as a system performance index for the current step based on the tracking error. According to the Bellman optimality, if a control action optimizes the cost-to-go function $J[k]$, then it optimizes the utility function r from k step and onward.

3.2 Adaptive Critic Design Control algorithm design

The block diagram of the proposed control solution is shown in Fig. 3, where the action NN is providing control signal to the MVAC SPS while the critic NN

approximates the cost-to-go function. In Fig. 3, the information flow of the NNs' inputs and outputs is illustrated using solid lines while the information flow for the NN updates is illustrated using dashed lines.
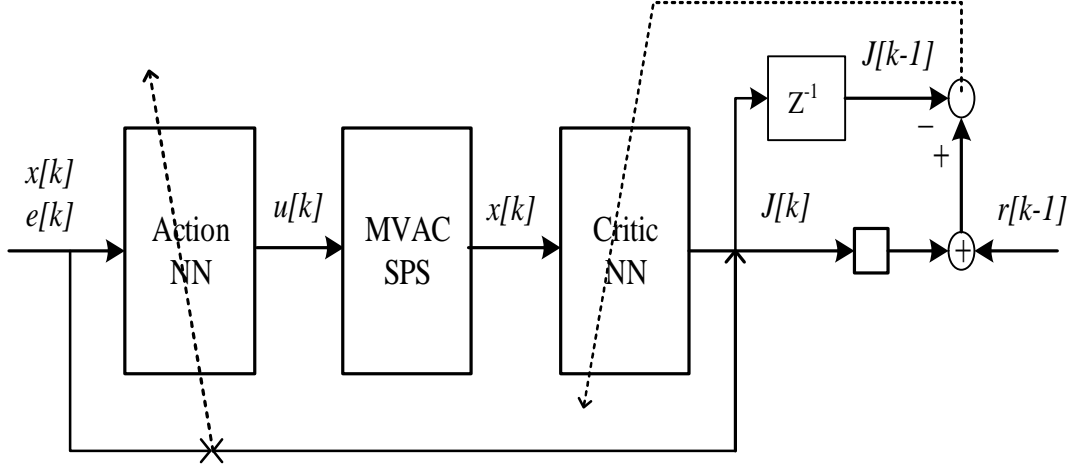
Figure 3 *Block diagram of the ACD-based control solution*

3.2.1: Design of Critic NN

In this paper, a critic NN is utilized to approximate the target cost-to-go function $J[k]$. Normally, the actual value of the kth step of $J[k]$ is unachievable in an online learning framework. Therefore, the critic NN needs to be tuned online in order to guarantee that the output of the critic NN approximately converges to the true $J[k]$.

Based on the approximation property of NNs, the optimal cost-to-go function $J^*[k]$ can be estimated by the critic NN with arbitrarily small approximation error $v_c(x[k])$ as

$$J^*[k] = W_c^T[k]\Phi_c(x[k]) + v_c(x[k]) \tag{7}$$

where W_c is the target weights of the critic NN.

Considering the fact that the target weights of the critic NN are unknown, the actual NN weights have to be updated online, and its actual output can be expressed as

$$\hat{J}[k] = \hat{W}_c^T[k]\Phi_c(x[k]) \tag{8}$$

12

where $\hat{W}_c$ is the approximation of W_c, and the approximation error is defined as

$$\varepsilon_c[k] = (\hat{W}_c[k] - W_c)^T \Phi_c(x[k]) \tag{9}$$

Then the prediction error of the critic NN or the Bellman error [21] can be formulated as a function of two successive predicted values of the cost-to-go function $\hat{J}[k]$.

$$e_c[k] = \times \hat{J}[k] - \hat{J}[k-1] + r[k] \tag{10}$$

Accordingly, the utility function is defined in the standard quadratic form as **Error! Reference source not found.**.

$$
\begin{aligned}
r[k] &= (\mathbf{y}[k] - \mathbf{y_d}[k])^T Q(\mathbf{y}[k] - \mathbf{y_d}[k]) + u^T[k]Ru[k] \\
&= \begin{bmatrix} f[k] - f_d[k] \\ V_C[k] - V_d[k] \end{bmatrix}^T Q \begin{bmatrix} f[k] - f_d[k] \\ V_C[k] - V_d[k] \end{bmatrix} + \begin{bmatrix} P_G[k] \\ I_C[k] \end{bmatrix}^T R \begin{bmatrix} P_G[k] \\ I_C[k] \end{bmatrix}
\end{aligned} \tag{11}
$$

where Q and R are diagonal positive definite matrices. The second part of **Error! Reference source not found.** is a standard term representing control effort that could be regarded as the energy consumption.

The objective function of the critic NN to be minimized can be defined as a quadratic function of the prediction error.

$$E_c[k] = \frac{1}{2} e_c^T[k]e_c[k] = \frac{1}{2} e_c^2[k] \tag{12}$$

After combining**Error! Reference source not found.**,**Error! Reference source not found.** and**Error! Reference source not found.**, the gradient of the critic NN weight updating rule can be obtained using the chain rule as

$$
\begin{aligned}
\Delta \hat{W}_c[k] &= -\Gamma_c \frac{\partial E_c[k]}{\partial \hat{W}_c[k]} = -\Gamma_c \frac{\partial E_c[k]}{\partial e_c[k]} \frac{\partial e_c[k]}{\partial \hat{J}[k]} \frac{\partial \hat{J}[k]}{\partial \hat{W}_c[k]} \\
&= -\Gamma_c \times \Phi_c(x_c[k])e_c[k]
\end{aligned} \tag{13}
$$

where r_c $(0 < r_c < 1)$ is a positive learning gain.

Finally, the critic NN output weights updating rule can be given as **Error! Reference source not found.** by combining**Error! Reference source not found.**.

$$\hat{W}_c[k+1] = \hat{W}_c[k] - r_c \mathsf{x} \Phi_c(x[k])(\mathsf{x}\,\hat{J}[k] - \hat{J}[k-1] + r[k]) \tag{14}$$

3.2.2: Design of Action NN

The action NN functions as an online learning-based optimal controller for the MVAC SPS. The purpose of the action NN design is to track the desired references and to minimize the cost function simultaneously.

By definition, the tracking error dynamics under control can be represented as.

$$\begin{aligned} e[k+1] &= x[k+1] - x_d[k+1] \\ &= f(x[k]) + g(x[k])u[k] + d[k] - x_d[k+1] \end{aligned} \tag{15}$$

From **Error! Reference source not found.**, the desired feedback control law can be given as

$$u_d[k] = g(x[k])^{-1}(-f(x[k]) + x_d[k+1] + le[k]) \tag{16}$$

where $l \in 2 \times 2$ is a design matrix selected such that the tracking error $e[k]$ converges to zero asymptotically.

Since the exact system dynamics is assumed to be unavailable, the control signal $u_d[k]$ cannot be obtained directly. Therefore, the approximation capability of NN is adopted to approximate the desired control signal as

$$u_d[k] = W_a^T \Phi_a(x_a[k]) + \mathsf{v}_a(x_a[k]) \tag{17}$$

where W_a is the desired weights of the action NN, $x_a[k] = [x[k] \quad x_d[k] \quad x_d[k+1]]^T$ is the action NN input vector, and $\mathsf{v}_a(x_a[k])$ is the NN reconstruction error.

Considering the fact that the target weights of the action NN are unknown, the actual NN weights have to be tuned online. The real-time output of the action NN can be expressed as

$$\hat{u}[k] = \hat{W}_a^T \Phi_a(x_a[k]) \tag{18}$$

where $\hat{W}_a$ is the approximation of W_a.

Substituting **Error! Reference source not found.** and **Error! Reference source not found.** into **Error! Reference source not found.** yields the closed-loop tracking error dynamics

$$e[k+1] = y[k+1] - y_d[k+1] = le[k] + g(x[k])'_a[k] + d_a[k] \tag{19}$$

$$'_a[k] = (\hat{W}_a[k] - W_a)^T \Phi_a(x_a[k]) \tag{20}$$

$$d_a[k] = -g(x[k])v_a(x_a[k]) + d[k] \tag{21}$$

For the purpose of tracking the desired references and minimizing cost function, the error for the action NN can be formulated as a function of the estimation error $'_a[k]$ and the critic signal $\hat{J}[k]$. Thus, by defining the cost function vector as $\bar{J}[k] = \begin{bmatrix} \hat{J}[k] & \hat{J}[k] \end{bmatrix}^T$, the action NN error can be given as

$$e_a[k] = \sqrt{g(x[k])}'_a[k] + (\sqrt{g(x[k])})^{-1}\bar{J}[k] \tag{22}$$

Thereafter, the objective for online tuning of the action NN is to minimize the error defined as

$$E_a[k] = \frac{1}{2}e_a^T[k]e_a[k] \tag{23}$$

By combining **Error! Reference source not found.**, **Error! Reference source not found.**, **Error! Reference source not found.**, and

15

Error! Reference source not found., the updating rule for the action NN weights can be written by utilizing the steepest descent method and the chain rule as

$$\Delta \hat{W}_a[k] = -\Gamma_a \frac{\partial E_a[k]}{\partial \hat{W}_a[k]} = -\Gamma_a \frac{\partial E_a[k]}{\partial e_a[k]} \frac{\partial e_a[k]}{\partial '_a[k]} \frac{\partial '_a[k]}{\partial \hat{W}_a[k]}$$
$$= -\Gamma_a \Phi_a(x_a[k])(g(x[k])'_a[k]) + \bar{J}[k])^T$$
$$= -\Gamma_a \Phi_a(x_a[k])(e[k+1] - le[k] + \bar{J}[k])^T$$

(24)

where $\Gamma_a (0 < \Gamma_a < 1)$ is the adaptation gain of the action NN.

Thus, the updating rule of the action NN weights can be further rephrased as

$$\hat{W}_a(k+1) = \hat{W}_a[k] - \Gamma_a \Phi_a(x_a[k])(e[k+1] - le[k] + \bar{J}[k])^T$$

(25)

Finally, the stability of the closed-loop system with ACD-based control algorithm can be guaranteed in following theorem.

Theorem 1: Consider the discrete-time SPS system given by (3). Let the control signal be provided by the action NN **Error! Reference source not found.**, with the critic NN **Error! Reference source not found.**. Further, let the weights of the action NN and the critic NN be tuned by **Error! Reference source not found.** and **Error! Reference source not found.** respectively. Then, the closed loop tracking error $e[k]$, and the NN weight estimate errors of the action and critic NNs, $'_a[k]$ and $'_c[k]$ are uniformly ultimately bounded.

Proof: The proof is similar to that in [22] and thus omitted here for simplicity purpose.

3.3 Control design Implementation

The implementation of the ACD based optimal controller is illustrated in Fig. 4. The control signals, P_M and I_C, generated by aforementioned ACD control law, are used as control references for the inner control loops.

Since the control law only produces the overall generation P_M, generation dispatch process is needed to assign generation tasks to the multiple generators within the SPS. Energy efficiency is important for the distance and duration that a ship can travel. For generators of different types, main and auxiliary, the generation cost functions are different. Thus, the generation task should be optimally dispatched within multiple generators. Considering that P_M has brought supply-demand balance into consideration, only local constraints such as generation bounds need to be considered. To improve reliability and survivability, the distributed generation control algorithm proposed in [30] can be revised and introduced. The charging current reference can be easily tracked by PI (Proportional integral) or hysteresis based controllers.
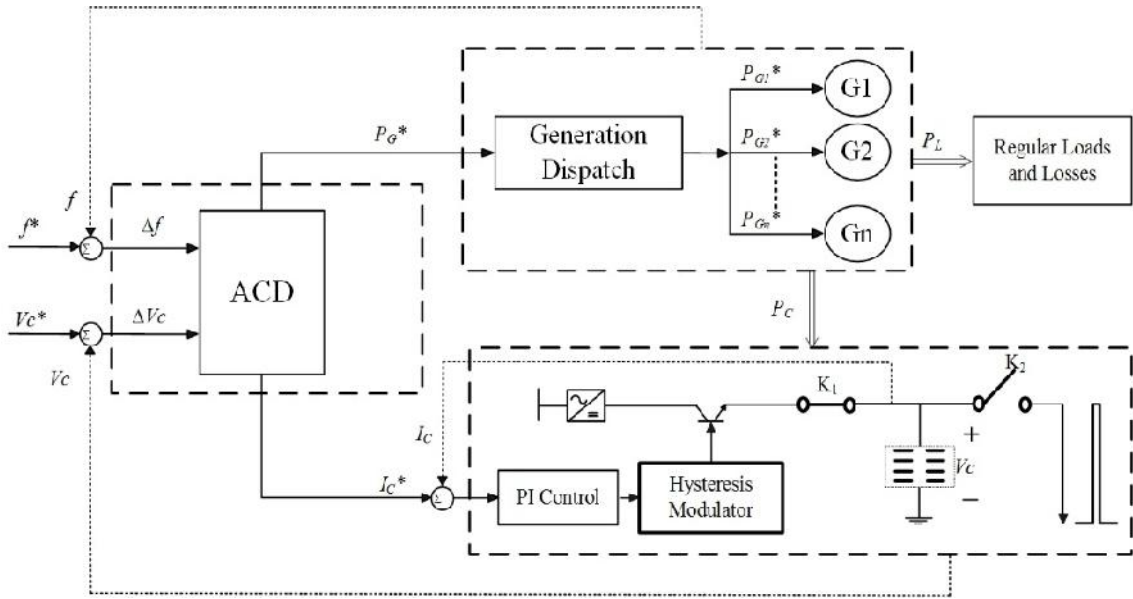
Figure 4 *Schematic diagram of the control*

3.4 Simulation and Experiment studies

The developed algorithm has been tested with SPS models of different size and complexity. The algorithm was first tested with the simplified mathematical SPS model formulated in **Error! Reference source not found.** and

Error! Reference source not found.. Then, it was tested with a detailed single-generator SPS model through PHIL simulation. Finally, a detailed multiple-generator SPS model is used to test the designed algorithm through real-time simulation. In this way, the performance of the designed algorithm can be evaluated accurately.

Since directly setting the reference of V_C to its final value ($V_C{}^*$) might create large disturbance during the initial stage of charging, the profile-based $V_C{}^*$ setting algorithm proposed in [18] is employed. The profile-based reference setting algorithm can avoid significant changes in reference signal and can guarantee charging completion within designated time under ideal conditions. The controller parameters are initially set as: diagonal positive definite matrices Q and R are set to be *[1 0; 0 1]* and *[1 0; 0 1]*, respectively; discount factor   for this infinite-horizon problem is *0.9*; the design matrix l, which is used to force the tracking error to converge to zero asymptotically, is selected as *[0.0005 0; 0 0.0005]*; the adaptation gains for the action NN and critic NN are *0.5* and *0.1*, respectively; the hidden layer of the action and critic NNs has 10 neurons, i.e., $n_a=n_c=10$.

3.4.1 Test with simplified mathematical model through offline simulation

Before testing the proposed control algorithm under unmodeled dynamics, it is first evaluated with a second-order mathematical model formulated using **Error! Reference source not found.** and **Error! Reference source not found.**. The goal is to charge V_C from 0 volts to 400 volts, which means 161.6 kJ will be accumulated in a 2.02 F supercapacitor within 23 seconds. The simulation results are provided as followed.

In Fig. 5, one can see that the charging current increases much faster at the beginning than at the end. Since $P_C=V_CI_C$, I_C does not need to be big during later stage of charging due to the increase of V_C. There is neither over-charging nor oscillation at the end of the charging process.

As it can be seen in Fig. 6, the tracking performance of V_C keeps improving and is fully converged before the designated time. This means the charging can be completed as expected. However, charging process cannot be completed on time under significant and durative increases of P_L, unless load shedding were deployed. In Fig. 6, one can see that the voltage tracking performance during the initial charging stage (0 s   t   5 s) is not that good. This is because the objective of the control algorithm is to minimize the tracking error for both f and V_C. Initially, the control of V_C is compromised to well regulate f, as shown in Fig. 7.

As shown in Fig. 8, initial P_M is not able to meet the charging demand. To maintain the supply-demand balance, the rotational potential energy is released to the system. That is why noticeable yet acceptable frequency drop is observed during that stage.
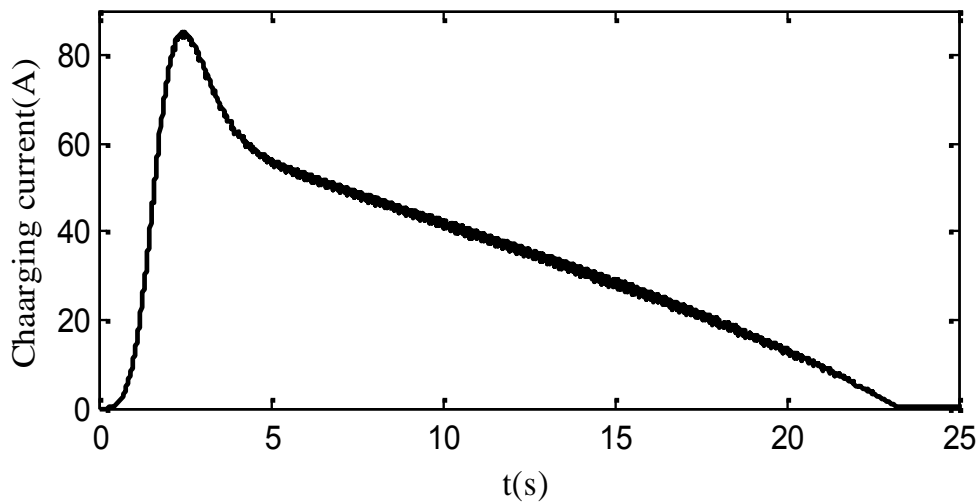
Figure 5 I_C *of system response with the simplified single generator SPS model.*

19
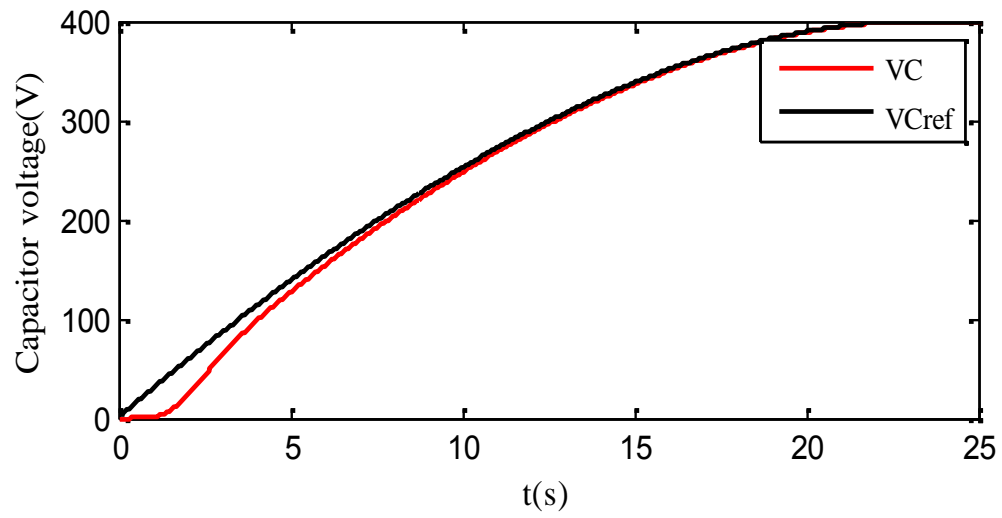
Figure 6 *V$_C$ of system response with the simplified single generator SPS model.*
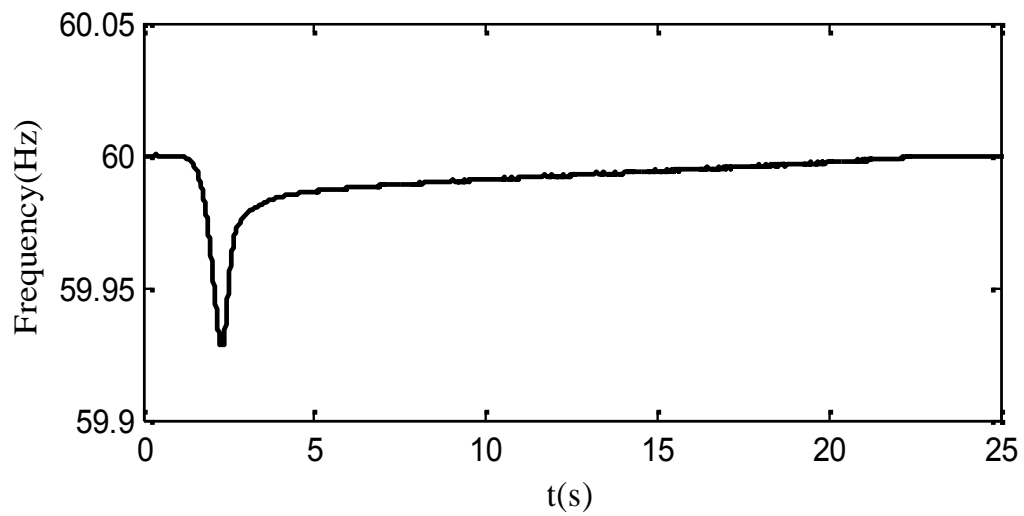
Figure 7 *Frequency of system response with the simplified single generator SPS model.*
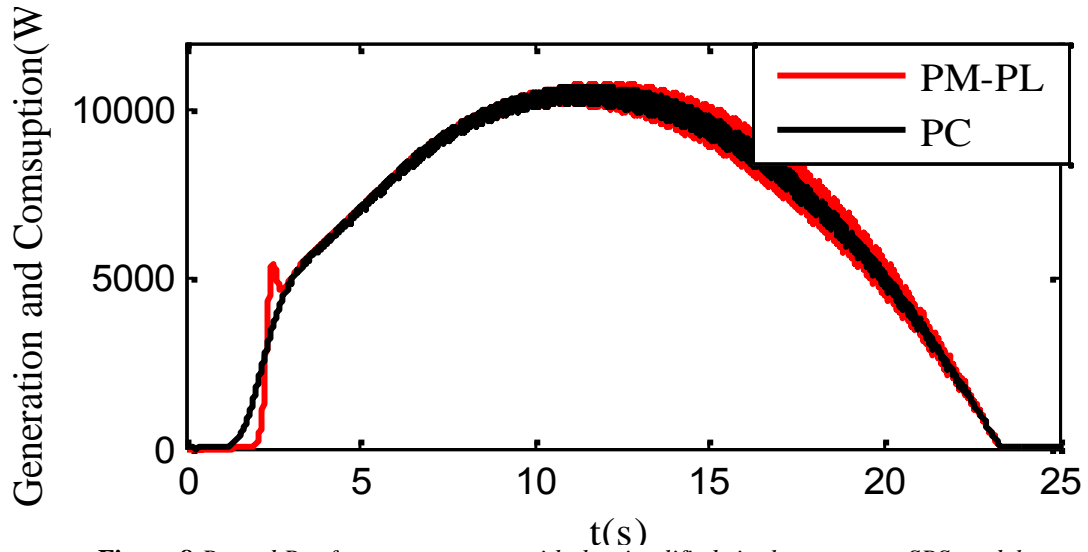
Figure 8 *P_M and P_C of system response with the simplified single generator SPS model.*

3.4.2 Test with detailed single-generator SPS model through PHIL simulation

To test the designed control algorithms, it is desirable to implement the algorithms using hardware controllers to control physical devices. However, full-hardware experimentation is beyond the capability of most research institutions. The closest way is to test the algorithms through PHIL simulation. During the test, the proposed control algorithm is implemented using DSP controller to control the subsystems accurately emulated. The concept is illustrated in Fig. 9.

21
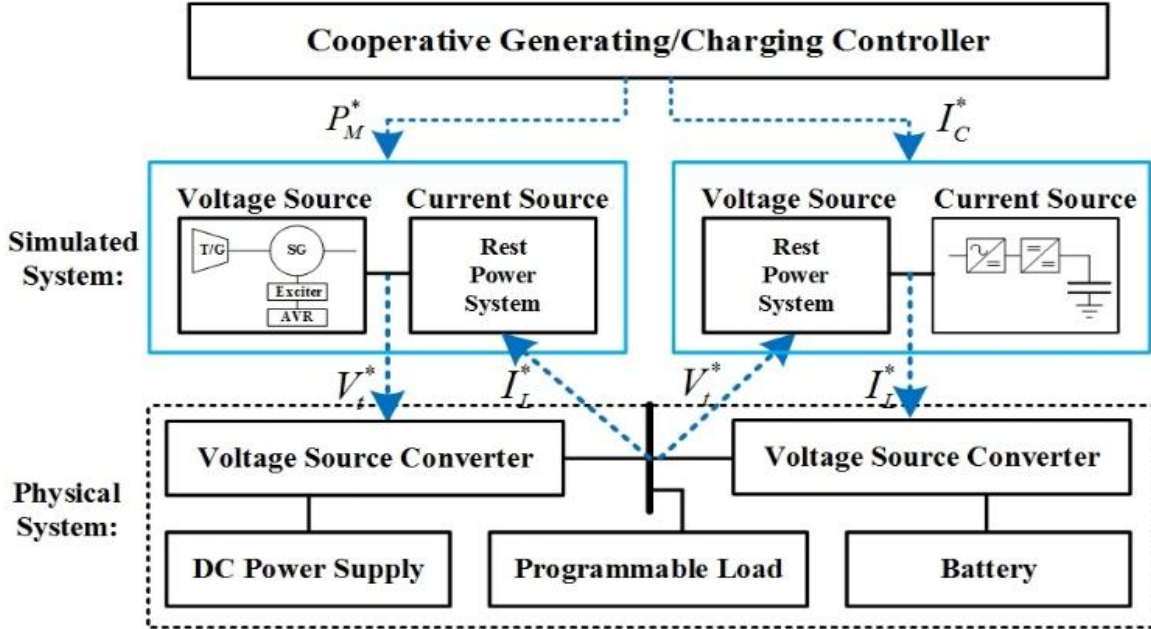
Figure 9. Concept of PHIL simulation

The PHIL simulation platform is consisted of an emulated SG and an emulated supercapacitor. To emulate a physical system, two subsystems, one for signal calculation and one for signal realization, are needed. During signal calculation, the system to emulate is modeled as a voltage source, which is connected to a current source model representing the rest system. The model is simulated in real-time to generate the voltage signal for a voltage source converter (VSC) to realize. The interaction of the two VSCs for SG and supercapacitor emulations will change the current and voltage at the coupling point. The measured current and voltage are then fed to the simulated models to update the simulation for next round of signal calculation.

During PHIL simulation, the SG is simulated with the one-axis model [31] with turbine-governor, automatic voltage regulator, and exciter. The equations and parameters can be found in [32][33]. As illustrated in Fig. 10, the charging circuit for the supercapacitor is consisted of an active AC-DC converter and a buck converter. The parameters of the circuit are provided in Table I. An average model for the charging

circuit is simulated with a DSP controller during PHIL emulation. The modular/decoupled way of subsystem emulation makes it easier for large-scale system emulation. The ideal transformer model is used for PHIL simulation due to its simplicity and effectiveness [26].
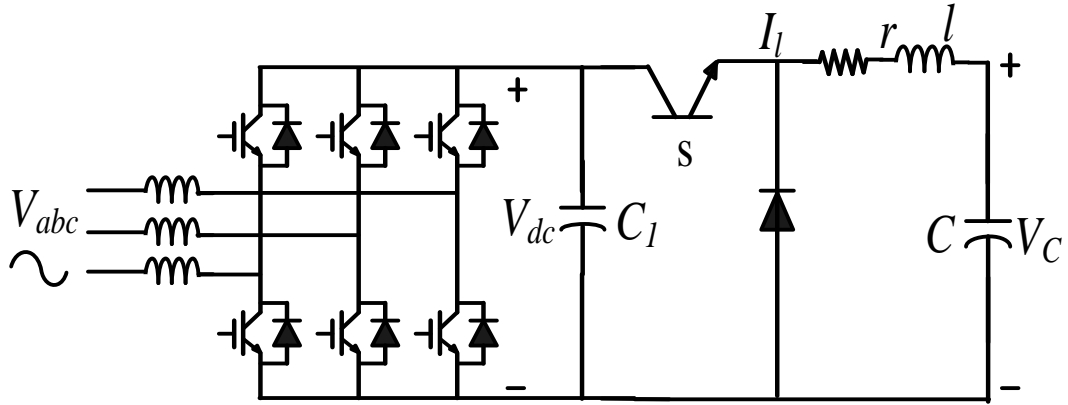
Figure 10 *Charging circuit for supercapacitor*

Table 1 PARAMETERS FOR CHARGING CIRCUIT

Parameter	Value	Description
r	0.1 ohm	Output resistance
l	5 mH	Output inductance
C_l	4.7 mF	Input filter capacitance
C	2 F	Supercapacitor (emulated)
V_{ABC}	208 V	Nominal Voltage
V_{DC}	330 V	DC-link voltage

The PHIL simulation of the 3 kW single-generator MVAC SPS shown in Fig. 2 is illustrated in Fig. 11. Two inverters of a renewable microgrid testbed were used to emulate the generator and the supercapacitor, respectively. The input to the emulated generator is provided by a DC power supply. The output of the charging circuit for the emulated 2 F supercapacitor is absorbed by a pack of batteries. In addition, a variable AC load was used for initialization and then emulation of P_L. The ramp rates of the single-generator and constraints of the supercapacitor are set in Table II.

Table 2 CONTROL CONSTRAINTS

Generator	P_G	Supercapacitor	I_C	V_C
Ramp-up rate	0.06 kW/s	Upper bound	6 A	85 V
Ramp-down rate	-0.06 kW/s	Lower bound	-6 A	50 V
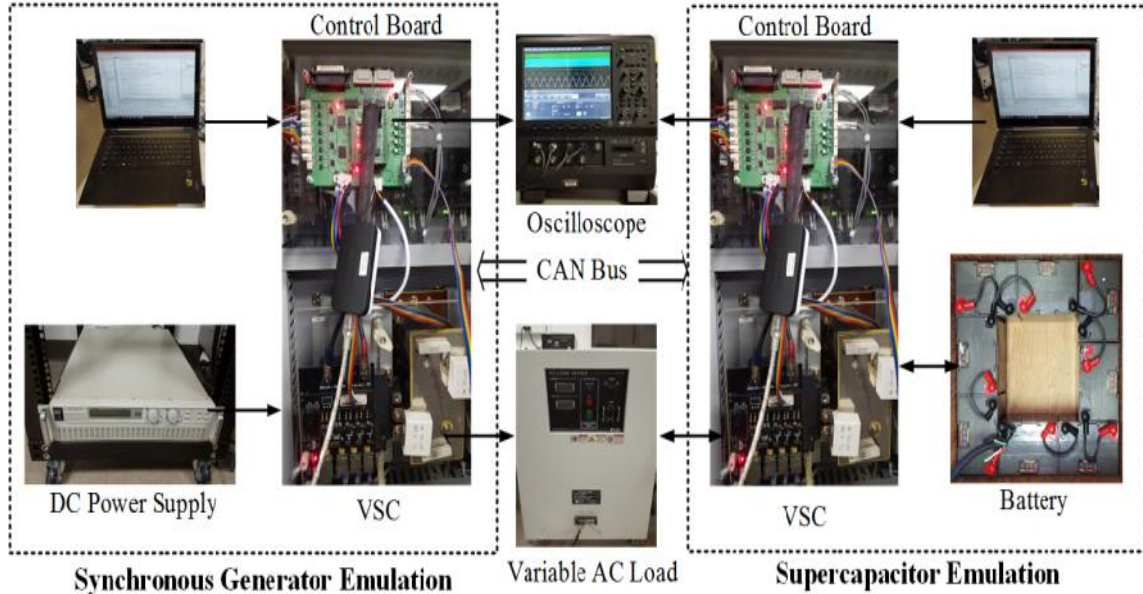
Figure 11 *Experiment implementation SPS system*

Two DSP control boards are used for real-time simulation of the subsystems and control of the VSCs. The sampling time for DSP implementation was 100 μs and the two control boards communicate with each other through CAN bus and the communication speed is 25 kbits/s. The proposed cooperative control algorithms were implemented on both control boards. Before the algorithms were implemented in *C* for hardware implementation, they were thoroughly tested through Simulink-based offline simulation. Since we know everything about the microgrid tested, hardware implementation of the algorithms did not give us too much trouble.

Based on the parameters of the physical system, the control objective is to charge 4.725kJ of energy to the emulated supercapacitor within 23 seconds. The charging

24

process starts at 5 seconds. During the process, V_C will increase from 50 V to 85 V. The PHIL simulation results of the proposed algorithm is summarized in Fig. 12. From V_C response, one can see that the control objective has been realized. I_C converges to zero immediately after the emulated supercapacitor gets fully charged without the undesirable overcharge or oscillation. The mismatch between V_C and V_C^* is to balance the control of f. Even though oscillation of f persists for a few seconds after charging, the magnitude is very small. Since the detailed model of the emulated SPS is much more complicated than the 2nd order model used for control, good PHIL simulation results demonstrate the effectiveness of the developed model and control algorithm.
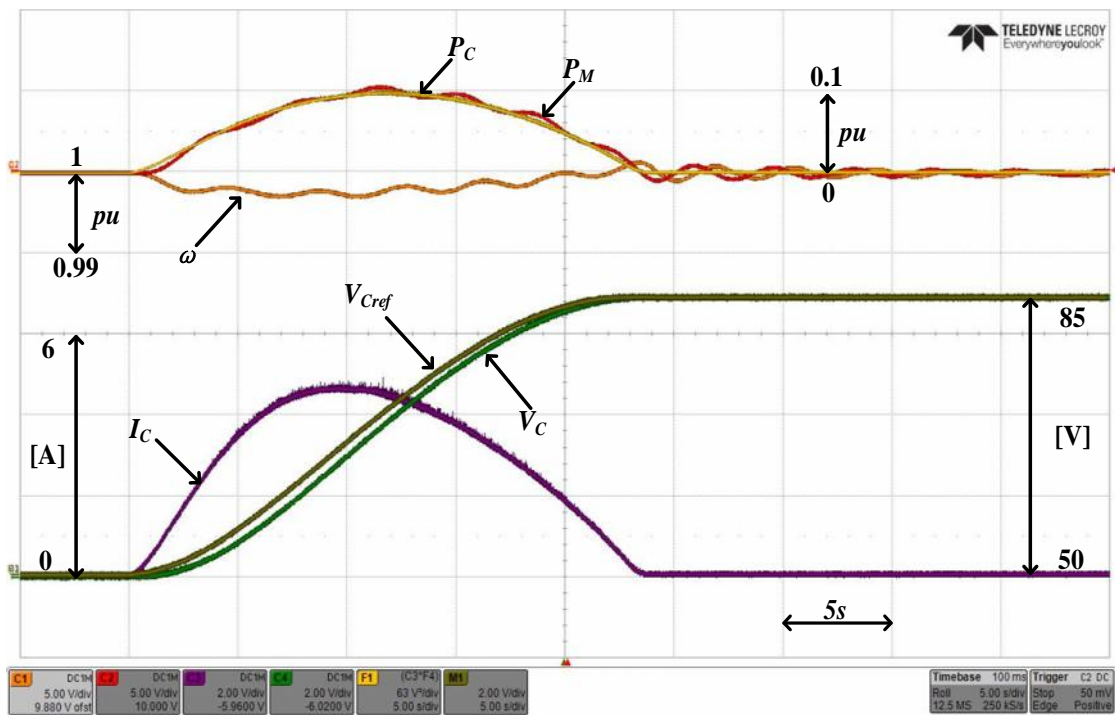
Figure 12 *Experiments responses based on power hardware in the loop*

3.4.3 Test with detailed multiple-generator SPS model on real-time simulation

The proposed algorithm is also tested with a multiple-generator MVAC SPS model through real-time digital simulation. Parameters of the SPS can be found in [2][34]. The

25

simulation is performed with the OPAL-RT real-time simulator in our lab. During

simulation, 3 out of the 5 unlocked CPS cores are used. The simulator can simulate the

SPS model and implement the designed algorithm in real-time without overruns. The

control objective is to charge an 18.75F supercapacitor from 2000 V to 3400 V in 23

seconds. During control implementation, the generations of the two auxiliary generators

are held constant, and the charging demand was shared evenly between the two main

generators. As shown in Fig. 13-16, similar performance like the previous two tests are

observed. The real-time simulation results demonstrate the effectiveness of the designed

algorithm.
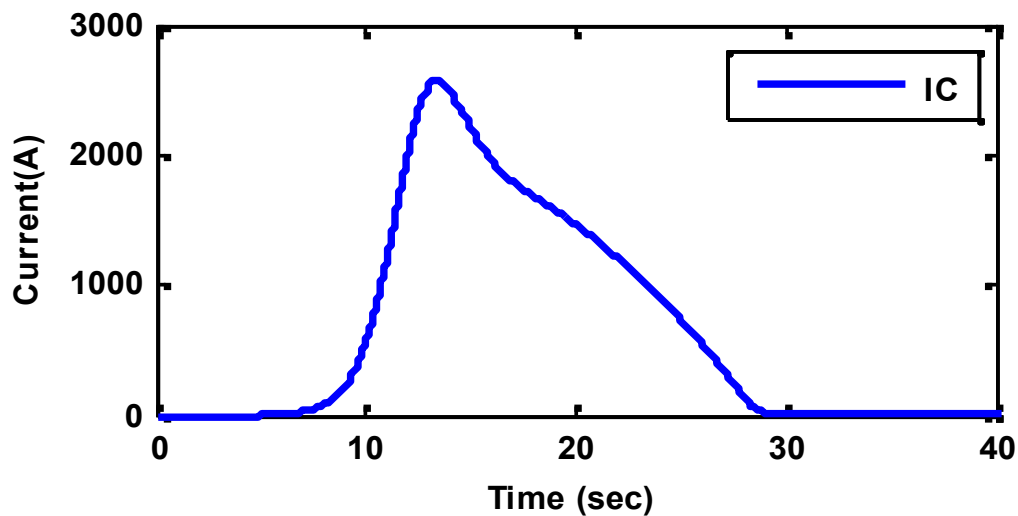
Figure 13 *I_C of system response with multiple generators SPS model*
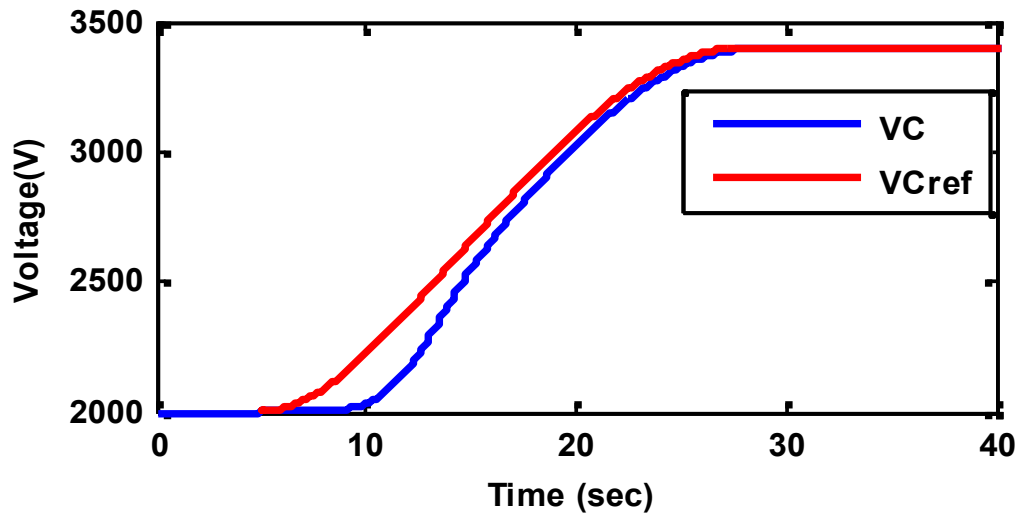
Figure 14 V_C and V_C^* of system response with multiple generators SPS model
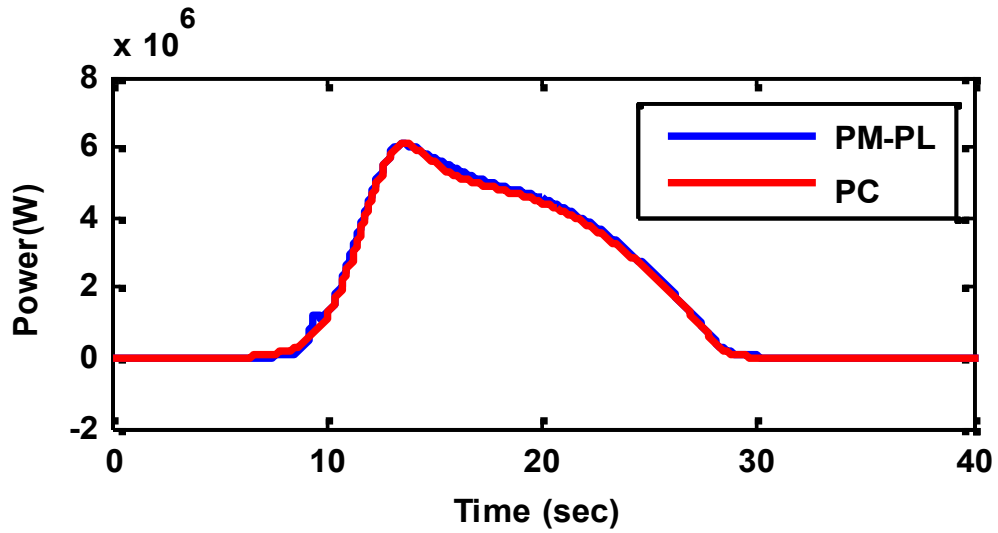
Figure 15 P_M and P_C of system response with multiple generators SPS model
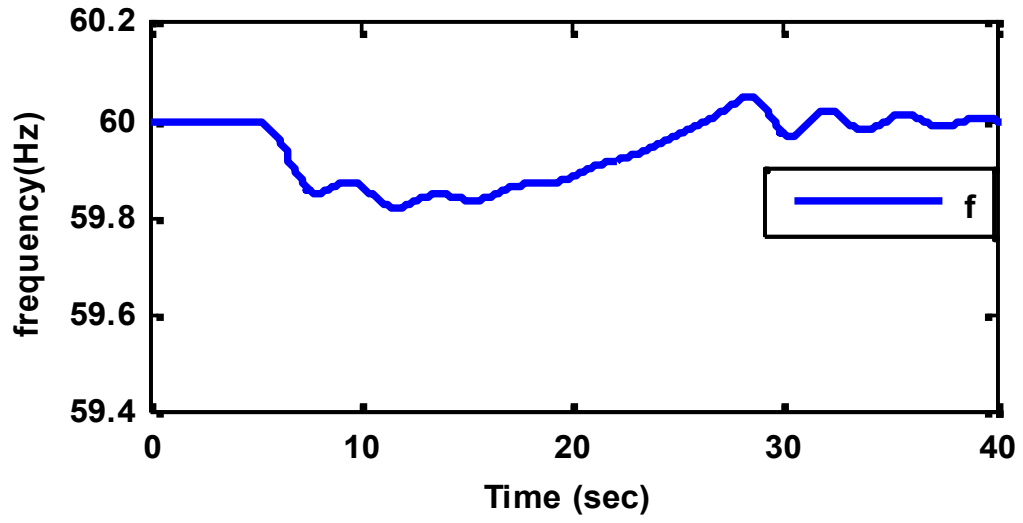
Figure 16 *Frequency of system response with multiple generators SPS model.*

4. Conclusion and Future Work

PPL accommodation in SPS is an important but not well studied problem. Through ESS installation, the huge transient demand of PPL can be transformed into a mild one by charging the ESS within a decent amount of time. To realize fast charging of the ESS and minimize disturbances during charging, generation control and charging control in the SPS should be well coordinated. In this paper, an ACD-based near optimal control design is presented based on a simple but effective SPS model. The algorithm is tested with both detailed single- and multiple-generator SPS models and tested through both real-time digital and power hardware-in-the-loop simulations. Simulation results demonstrate the effectiveness of the developed model and control algorithm.

In the future, advanced distributed control algorithms can be designed based on detailed model of the SPS.

References

[1]M. Bash, R. R. Chan, J. Crider, C. Harianto, J. Lian, J. Neely, S. D. Pekarek, S. D. Sudhoff, and N. Vaks, "A Medium Voltage DC Testbed for ship power system research," *2009 IEEE Electr. Sh. Technol. Symp.*, pp. 560–567, Apr. 2009.

[2]ESRDC Report, "Documentation for Notional Baseline System Models Version 0.2 DRAFT," 2012.

[3]J. J. a. van der Burgt, P. van Gelder, and E. van Dijk, "Pulsed power requirements for future naval ships," *Dig. Tech. Pap. 12th IEEE Int. Pulsed Power Conf.*, vol. 2, pp. 1357–1360, 1999.

[4]X. Feng, "A multi-agent system framework for real-time electric load management in MVAC all-electric ship power systems," *IEEE Trans power syst*, vol. 30, no. 3, pp. 1327–1336, 2015.

[5]S. Kulkarni and S. Santoso, "Impact of pulse loads on electric ship power system: With and without flywheel energy storage systems," *IEEE Electr. Sh. Technol. Symp.*, pp. 568–573, Apr. 2009.

[6]V. Salehi, B. Mirafzal, and O. Mohammed, "Pulse-load effects on ship power system stability," in *Proc. 36th Annu. Conf. on IEEE Ind. Electron.Soc.*, 2010, pp. 3353–3358.

[7]M. Steurer, M. Andrus, J. Langston, L. Qi, S. Suryanarayanan, S. Woodruff, and P. F. Ribeiro, "Investigating the Impact of Pulsed Power Charging Demands on Shipboard Power Quality," *IEEE Electr. Sh. Technol. Symp.*, pp. 315–321, May 2007.

[8]L. N. Domaschk, A. Ouroua, R. E. Hebner, O. E. Bowlin, and W. B. Colson, "Coordination of Large Pulsed Loads on Future Electric Ships," *IEEE Trans. Magn.*, vol. 43, no. 1, pp. 450–455, Jan. 2007.

[9] F. Scuiller, "Simulation of an energy storage system to compensate pulsed loads on shipboard electric power system," *IEEE Electr. Sh. Technol. Symp.*, pp. 396–401, Apr. 2011.

[10] F. Scuiller, "Study of a supercapacitor Energy Storage System designed to reduce frequency modulation on shipboard electric power system," *IECON 2012-38th Annu. Conf. IEEE*, pp. 4054–4059, 2012.

[11] A. T. Elsayed, S. Member, and O. a Mohammed, "Distributed Flywheel Energy Storage Systems for Mitigating the Effects of Pulsed Loads," *PES Gen. Meet. Conf. Expo.*, pp. 1–5, 2014.

[12] A. Mohamed, V. Salehi, and O. Mohammed, "Real-time energy management algorithm for mitigation of pulse loads in hybrid microgrids," *IEEE Trans. Smart Grid*, vol. 3, no. 4, pp. 1911–1922, 2012.

[13] P. F. Ribeiro, B. K. Johnson, M. L. Crow, A. Arsoy, and Y. Liu, "Energy storage systems for advanced power applications," *Proc. IEEE*, vol. 89, no. 12, pp. 1744–1756, 2001.

[14] J. Mcgroarty, J. Schmeller, R. Hockney, S. Member, and M. Polimeno, "Flywheel Energy Storage System for Electric start and an All-Electric Ship," in *ieee electrical ship technologies symposium*, 2005, pp. 400–406.

[15] B. Vural and C. Edrington, "A novel inductive-capacitive pulse forming circuit for pulse power load applications," *IECON 2012-38th Annu. Conf. IEEE, Ind. Electron. Soc.*, pp. 4446–4450, 2012.

[16] S. D. Sudhoff, "Currents of change," *IEEE Power and Energy Mag.*, pp. 30–37, July–Aug, 2011.

[17]   E. Cassimere, B., Valdez, C. R., Sudhoff, S., Pekarek, S., Kuhn, B., Delisle, D., & Zivi, "System impact of pulsed power loads on a laboratory scale integrated fight through power (IFTP) system," *Electr. Sh. Technol. Symp.*, pp. 176–183, 2005.

[18]   J. M. Crider and S. D. Sudhoff, "Reducing Impact of Pulsed Power Loads on Microgrid Power Systems," *IEEE Trans. Smart Grid*, vol. 1, no. 3, pp. 270–277, Dec. 2010.

[19]   P. J.Werbos, "Advanced forecasting methods for global crisis warning and models of intelligence," *Gen. Syst. Yearb.*, vol. 22, pp. 25–38, 1977.

[20]   C. Z. G. With, "Integral Reinforcement Learning for Linear Completely Unknown Dynamics," *IEEE Trans Autom. Sci. Eng.*, vol. 11, no. 3, pp. 706–714, 2014.

[21]   J. Si, S. Member, and Y. Wang, "On-Line Learning Control by Association and Reinforcement," *IEEE Trans. Neural Netw*, vol. 12, no. 2, pp. 264–276, 2001.

[22]   Q. Yang and S. Jagannathan, "Reinforcement learning controller design for affine nonlinear discrete-time systems using online approximators.," *IEEE Trans. Syst. Man. Cybern. B. Cybern.*, vol. 42, no. 2, pp. 377–90, Apr. 2012.

[23]   D. Wang, D. Liu, and H. Li, "Policy Iteration Algorithm for Online Design of Robust Control for a Class of Continuous-Time Nonlinear Systems," *IEEE Trans Autom. Sci. Eng.*, vol. 11, no. 2, pp. 627–632, 2014.

[24]   H. Bevrani, *Robust Power System Frequency Control*. Springer, 2008.

[25]   G. Andersson, *Dynamics and Control of Electric Power Systems*. Zurich: EEH-Power Systes Laboratory, ETH Zurich, 2012.

[26]   A. R. Barron, "Universal Approximation Bounds for Superposition of a Sigmoid Function," *IEEE Trans. Inf. Theory*, vol. 39, no. 3, pp. 930–945, 1993.

[27] B. Igelnik and Y. H. Pao, "Stochastic choice of basis functions in adaptive function approximation and the functional-link net," *IEEE Trans. Neural Netw.*, vol. 6, no. 6, pp. 1320–1329, Jan. 1995.

[28] Q. Wei and D. Liu, "A Novel Iterative -Adaptive Dynamic Programming for Discrete-Time Nonlinear Systems," *IEEE Trans. Neural Networks Learn. Syst.*, vol. 11, no. 4, pp. 1176–1190, 2014.

[29] W. Liu, G. K. Venayagamoorthy, and D. C. Wunsch, "A heuristic-dynamic-programming-based power system stabilizer for a turbogenerator in a single-machine power system," *IEEE Trans. Ind. Appl.*, vol. 41, no. 5, pp. 1377–1385, 2005.

[30] W. Zhang and W. Liu, "Online Optimal Generation Control Based on Constrained Distributed Gradient Algorithm," *IEEE Trans. Power Syst.*, vol. 30, no. 1, pp. 35–45, 2015.

[31] M. N. Marwali and A. Keyhani, "Control of distributed generation systems - Part I: Voltages and currents control," *IEEE Trans. Power Electron.*, vol. 19, no. 6, pp. 1541–1550, 2004.

[32] P. W. S. M. A. PAI, *Power system dynamics and stability*, 1st ed. Prentice Hall, 1998.

[33] P.M. Anderson and A.A. Fouad, *Power System Control and Stability*, 2nd ed. WILEY-INTERSCIENCE, 1977.

[34] W. Im, C. Wang, L. Tan, W. Liu, and L. Liu, "Cooperative controls for pulsed power load accommodation in a shipboard power system," *IEEE Transactions on Power Systems* (http://dx.doi.org/10.1109/TPWRS.2016.2538323)

Vita

Liang Tan was born and raised in Zhuzhou, China. He received his bachelor and master degree from Northeastern University (CN) with Automation major in 2011 and Control Engineering major in 2013, respectively. In August 2013, he joined the group of Professor Wenxin Liu in NMSU (New Mexico State University) and then transferred to Lehigh University in January 2015. His research interests mainly include control of Microgrid and optimization of power system. He has extensive experience of power system and power electronics simulation, also he has many hands-on experience of analog and digital circuit design, and various applications with microcontroller.

He has two accepted papers, one paper is under review and another is under preparation.

1) Wonsang Im, Cheng Wang, **Liang Tan**, W. Liu, "Cooperative Controls for Pulsed Power Load Accommodation in a Shipboard Power System", *IEEE trans on power system*

2) **Liang Tan**, Qinmin Yang, Wonsang Im, W. Liu, "Adaptive Critic Design based Cooperative Control for Pulsed Power Loads Accommodation in Shipboard Power Systems", *IET generation, transmission & distribution*.